Pergamon

J. Aerosol Sci., Vol. 26, No. 8, pp. 1257–1279, 1995

0021-8502/95 $9.50 + 0.00

0021-8502(95)00045-3

LOCAL SIZE DISTRIBUTIONS OF PARTICLES DEPOSITED BY INERTIAL IMPACTION ON A CYLINDRICAL TARGET IN DUST-LADEN STREAMS

Daniel E. Rosner,* Pushkar Tandon and A. G. Konstandopoulos

High Temperature Chemical Reaction Engineering Laboratory, Department of Chemical Engineering, Yale University, New Haven, CT 06520-8286, U.S.A.

(*First received* 6 *July* 1994; *and in final form* 17 *May* 1995)

Abstract—We exploit recent developments on impinging single particle capture laws and rational correlations for inertial impaction on a circular cylinder in high Reynolds number crossflow [Israel and Rosner (1983) *Aerosol Sci. Technol.* **2**, 45–51; Wessel and Righi (1988) *Aerosol Sci. Technol.* **9**, 26–60] to predict the *local size distribution of particles deposited by impaction* on a cylindrical target when the mainstream particle suspension is "log-normal". Because of both the aerodynamics of selective impingement, and the nature of the sticking/rebound law, we show that the granular deposit particle size distribution (hereafter abbreviated $(PSD)_W$) is generally quite different from mainstream particle size distribution $(PSD)_\infty$, by so much that $(PSD)_W$ generally cannot be characterized accurately by single-mode log-normal distribution parameters. Apart from its relevance in correcting for systematic errors in aerosol sampling from high-speed streams, this local variation of the "granular deposit" PSD along with information on deposit morphology, must be known (in addition to the total mass accumulated per unit area) to predict, say, the loss in convective heat transfer rate associated with the growth of a fouling layer. Three distinct classes of single solid *particle capture laws* are considered: constant capture fraction (independent of impinging particle velocity and angle of incidence), "on-off" capture behavior expected for impaction on a clean, particle-free, smooth solid surface, and particle capture on a dry, sufficiently thick, granular deposit. Our $(PSD)_W$ results are cast in terms of following accessible dimensionless parameters: sensitivity of capture fraction to particle incident velocity and angle, ratio of mainstream velocity to the critical (threshold) velocity for particle rebound (at, say, normal incidence), ratio of mean particle size in the mainstream to the critical size required for impaction on a cylindrical target in crossflow, spread of log-normal mainstream particle size distribution, and the characteristic "slip" Reynolds number for the critical size particle in the mainstream.

NOMENCLATURE

c	constant in equation (9) (= 0.158)
$C_\infty\{v\}$	normalized log-normal distribution function, equation (18)
C_{dep}	normalized distribution function in the deposit
$\bar{C}_{dep}$	pooled particle size distribution function in the deposit over upwind target surface
C_D	quasi-steady particle drag coefficient; Section 2.3
d_p	particle diameter, $(6v/\pi)^{1/3}$
d_t	circular cylinder (target) diameter, Fig. 1
$\bar{D}_h$	Nusselt number-weighted dimensionless deposition rate
$(DR)_{ref}$	reference deposition rate; equation (30)
g	normalized (with respect to gas mainstream velocity) particle impingement velocity; Section 2.4
$\mathscr{H}$	Heaviside function (Section 2.2)
k_{dep}	thermal conductivity of the deposit
k_g	thermal conductivity of the gas
$n\{v\}$	particle number density distribution function (= dN_p/dv)
N_p	total particle number density
Nu_h	heat transfer Nusselt number (see e.g. Rosner, 1986); Section 4
Re	Reynolds number based on target cylinder diameter (= Ud_t/v)
Re_p	Reynolds number based on particle diameter (= Ud_p/v)
$Re_{p,cr}$	Reynolds number based on critical size particle
s	capture (sticking-) fraction upon local impaction
Sc	Schmidt number (= v/D)
Stk	particle Stokes number [= t_p/t_{flow} where $t_{flow} = (d_t/2)/U$]
Stk_{eff}	effective particle Stokes number (= $Stk \cdot \psi\{Re_p\}$)

*Author to whom correspondence should be addressed.

$\mathrm{Stk}_{\mathrm{eff,cr}}$ critical effective Stokes number for onset of inertial impaction ($\frac{1}{8}$ for circular cylinder at $\mathrm{Re}_t^{1/2} \to \infty$)
t_p particle stopping time (Stokes drag)
T absolute temperature
U gas mainstream velocity
v particle size (volume)
v_{crit} or v_{cr} volume of smallest particle capable of inertial impaction
$\bar{v}$ number mean particle volume
$\bar{v}_{dep}$ number mean particle volume in the deposit
v_g median volume of log-normal distribution of particles
V_p particle velocity at incipient impaction (Fig. 1)
$V_{p,cr}$ or V_{cr} critical velocity for rebound

Greek letters

β coefficients in curve-fit for particle angle of incidence
ε local void fraction in microgranular deposit
η or η_{loc} local impingement efficiency
η_{cap} target capture efficiency when $s = 1$
θ angle measured from the stagnation line (cf. Fig. 1)
θ_i local impingement angle with respect to local normal (cf. Fig. 1)
θ_{max} maximum angle at which impaction can occur (for a particular mainstream particle size)
μ dynamic viscosity of carrier gas
ν gas momentum diffusivity ($= \mu/\rho_g$) ("kinematic viscosity")
ξ dimensionless particle volume ($\equiv v/v_{crit}$)
$\bar{\xi}$ or $\bar{\xi}_\infty$ dimensionless mean particle volume ($\equiv \bar{v}/v_{crit}$)
$\bar{\xi}_{dep}$ dimensionless mean particle volume in the deposit
$\xi_{g,dep}$ dimensionless median volume of the log-normal particle size distribution in the deposit
ρ_g gas mass density
$\tilde{\rho}_p$ mass density of each particle
σ_g or $\sigma_{g,\infty}$ geometric standard deviation of log-normal distribution
$\sigma_{g,dep}$ geometric standard deviation of log-normal distribution in the deposit
ϕ_p particle volume fraction ($= \bar{v}N_p$)
Φ fraction of total mainstream population
ψ correction factor accounting for non-Stokesian drag behavior of particles for $\mathrm{Re}_p \geqslant O\{1\}$ (cf. Fig. 2b)
ω_p particle mass fraction $\tilde{\rho}_p\phi_p/(\rho_g + \tilde{\rho}_p\phi_p)$

Abbreviations, subscripts

BL gaseous boundary layer
crit critical (incipient impaction in prevailing environement)
crit or cr critical (at the transition between capture and rebound)
eff effective (corrected e.g. for non-Stokes drag; see Israel and Rosner, 1983)
g pertaining to gas
Gr pertaining to granular deposit
h pertaining to heat transfer
H pertaining to Heaviside ("bare" surface) capture/rebound law
lim limit
loc local
max maximum
n normal component (cf. Fig. 1)
$O\{\}$ order of magnitude
PSD particle size distribution
reb pertaining to rebound
ref reference value of
stick particles which are captured
wrt with respect to
w pertaining to the target surface ("wall")
∞ pertaining to mainstream
$\langle\,\rangle$ $\overline{(\,)}$
$\{\}$ argument of a function

1. INTRODUCTION

1.1. *Importance of the size distribution of deposited particles*

An understanding of the inter-relationships between the particle size distribution *in* a deposit and in the mainstream source "suspension" is clearly necessary in sampling applications. In such cases a target is deliberately introduced in a stream for the subsequent analysis of its captured particle sizes, morphology and/or chemistry. In the present paper, we initially consider the "direct" problem of predicting the particle size distribution in deposits at various positions along the surface of a circular cylinder target in crossflow

knowing: (a) the aerodynamics of the situation, (b) the mainstream particle size distribution (taken here to be log-normal) and (c) the particle capture (or rebound) law (Section 2.2). Our methods for solving the "inverse" problem—i.e. predicting $(PSD)_\infty$ from measurements of $(PSD)_W$ using our knowledge of the aerodynamics of impingement and the mechanics of particle rebound, are presented in Section 4.

In another important class of applications, initially clean heat exchanger surfaces exposed to high-temperature flowing suspensions—e.g. ash or soot particles in fossil fuel (oil) or coal combustion products, can acquire a sufficient fraction of this solid material to cause a noticeable decline in gas-side convective heat transfer performance associated with the local growth of a microgranular insulating "fouling" layer. The extent of degradation in heat transfer performance associated with the fouling layer not only depends on the total volume of particles deposited per unit area of target surface, but also on the local void fraction and size distribution of the particles in the deposit (see e.g. Rosner and Tandon (1995) and Section 4) (especially when the granular deposit morphology (solid fraction, etc.) and particle thermal properties are size dependent). We demonstrate here that this distribution ($(PSD)_W$) is often rather different from the particle size distribution in the mainstream, ($(PSD)_\infty$).

We recently developed and illustrated an efficient method to predict inertially induced particle *deposition rates* on cylindrical targets (Rosner and Tandon, 1995; Rosner *et al.*, 1994). In the present paper, we explicitly predict the local *deposit particle size distribution* in high-velocity particle-laden environments with log-normal particle size distribution in the mainstream. For this purpose, we exploit recent developments in the area of inertial impaction (Israel and Rosner, 1983; Wang, 1986; Wessel and Righi, 1988; Konstandopoulos *et al.*, 1993) and invoke recently developed single particle sticking (capture) laws for impaction on granular deposits (Konstandopoulos, 1991; Rosner *et al.*, 1992) and for impaction on clean smooth solid surfaces (Wang, 1986; Dahneke, 1971). For simplicity, we confine ourselves to engineering environments with negligible post-deposition particle sintering. We examine the canonical (and best-understood) geometry of a circular-cylindrical target in a spatially uniform, high Reynolds number cross-flow (cf. Fig. 1) and introduce a modest number of approximations to predict the local particle size distributions on the target surface. For convenience, our results will be cast in terms of following parameters: ratio of mainstream velocity U to threshold (critical) velocity for rebound from the solid surface ($V_{cr}\{v_{cr}\}$), ratio of mean particle size, $\bar{v}$, to the threshold size, v_{cr}, required for impaction on the circular cylinder target in the prevailing flow environment, spread, σ_g, of the mainstream particle size distributions (here assumed 'log-normal'), and the characteristic "slip" Reynolds number, $Re_{p,crit}$, for critical size particles in the mainstream. To our knowledge, there are no reported experimental measurements of particle size distribution on a cylinder in cross-flow, although Kim and Kim (1991) have reported particle size distributions in a deposit on a flat target under conditions where combined inertia and thermophoresis were the dominant mechanisms of deposition.

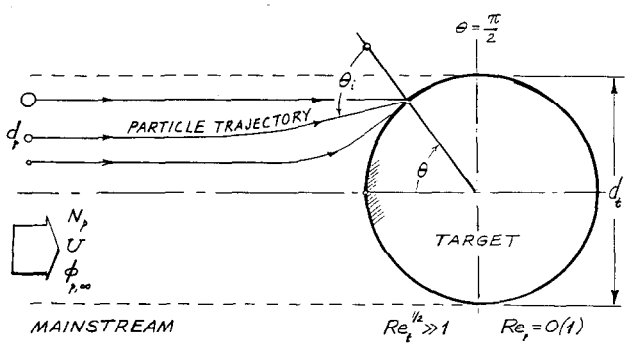

Fig. 1. Flow configuration and nomenclature; particle impaction/deposition on a circular cylinder in the crossflow of a particle-laden gas stream.

The present paper is structured as follows: in Section 2 we state the principal assumptions underlying our analysis of deposit particle size distributions, including a brief account of our choice of single particle capture laws and inertial impaction correlations. In Section 3, we present results for particle size distributions at several "sampling" positions on the upwind side of a circular cylinder in crossflow, for a log-normal size distribution of particles suspended in the mainstream. Section 4 includes comments on our results and their implications and offers a simple method which, in principle, solves the "inverse" problem of predicting (a predictable portion of) $(PSD)_\infty$ from $(PSD)_w$ data. Section 5 concludes with a summary of our principal findings and comments on extensions suggested by this work.

2. MATHEMATICAL MODEL AND FORMULATION

2.1. *Basic assumptions and cases explicitly considered*

By combining recent results on the impaction of initially suspended particles on the surface of a circular cylinder target in high Reynolds number spatially uniform crossflow, with single particle capture probability laws (when individual solid particles strike solid surfaces) it is possible to formulate/calculate the local size distribution of the captured particle population for such a target exposed to a flowing suspension of particles, say, log-normally "distributed" in particle size. To incorporate the essential phenomena in a simple manner without making unrealistic idealizations we make the following basic assumptions:

(A1) Local particle impaction frequencies, velocities, and angle of incidence can be calculated with sufficient accuracy from recently available correlations summarizing the results of individual suspended non-Brownian particle trajectories calculated for steady, inviscid flow of a uniform suspension past an isolated circular cylinder target (Fig. 1).

(A2) Important systematic departures from Stokes drag law (owing to the local particle slip† Reynolds numbers) can be adequately accounted for by using a modified ("effective") Stokes number which corrects for non-Stokesian drag in computing characteristic particle stopping time or distance in the prevailing viscous carrier gas (Israel and Rosner, 1983).

(A3) Even for impaction on granular deposits, suitable single particle capture probability laws at particular velocities and incidence angles can be invoked to predict capture fractions in engineering applications where suspended particles of different size arrive over a broad range of impact velocities and incidence angles.

(A4) "Rebounding" particles neither appreciably influence incoming particles, nor deposit in appreciable numbers upon re-impaction on the same target.

(A5) The mainstream population of suspended particles is approximately log-normal with respect to particle volume and, while the particle *mass loading*, ω_p, in the mainstream may not be very small, the *volume fraction*, ϕ_p, corresponding to the total particle number density N_p and mean particle volume $\bar{v}$ (i.e. $\phi_p = N_p\bar{v}$) *is* negligible.

(A6) On the scale of the *target* diameter the mainstream suspended particles are uniformly distributed in space and are individually negligible in size.

(A7) Particles in the deposit do not sinter and do not result in any evolution in local deposit particle size distribution subsequent to capture.

(A8) In low volume fraction systems where the suspended particles are large enough for inertial impaction to be the dominant mechanism of arrival and deposition, particle number densities are low enough for Brownian coagulation to be neglected in the target neighborhood.

(A9) Erosion (or resuspension) of particles in the deposit caused by subsequent impinging particles is neglected (however, see Section 2.2).

† Slip here is in the sense of the continuum multi-phase community and not that of aerosol science community (particles small compared to the molecular mean free path). Of course, in both cases the concern is systematic departures from Stokes drag law.

Some of these assumptions are critically examined by Rosner (1986), Tandon (1995), Rosner and Tandon (1995) and Rosner *et al.* (1995).

2.2. *Single particle capture probability laws*

Our purpose here is to *apply* the (admittedly incomplete) micromechanical theory of particle *capture sticking fraction*, s [which provides the functional form of s when particular projectile particles are directed at particular target materials (including granular deposits) at a known velocity V_p and angle of incidence θ_i (cf. the target outward normal)] to predict local particle capture rates and hence deposit particle size distributions for a cylindrical target immersed in a polydispersed suspension of such particles. We consider three distinct and idealized classes of single particle capture laws, as follows:

Constant capture fraction. The simplest "law," and one which has been used for many previous engineering estimates of fouling, is that capture occurs for some *constant fraction* $s \leqslant 1$ of impacts, irrespective of V_p and θ_i. This case will be called "constant capture fraction" and frequently labelled (and/or presented) for the limiting case $s=1$. When $s = \text{const} < 1$ then all $s = 1$ functions shown remain applicable because of our normalization procedure in reporting $(\text{PSD})_W$.

Perfect capture on clean solid surfaces only below threshold normal velocity. The second type of sticking law we consider is the individual particle capture behavior expected on a "clean" (particle-free) smooth surface (see e.g. Wang, 1986; Dahneke, 1971). In the simplest of such situations, an impacting particle is captured only if the normal velocity component, $V_{p,n}$, of the impacting particle is less than the size-dependent critical velocity, $V_{p,cr}\{v\}$, here taken to be an experimentally determined quantity. Thus, if the normal velocity component of the impacting particle is greater than this critical velocity, a rebound event occurs. We assume, further, that the rebounding particles do not appreciably influence incoming particles, nor deposit in appreciable numbers upon reimpaction downstream on the same target. Thus, the simplest sticking probability function for a particle impacting on a bare, smooth solid surface can be conveniently written:

$$s = \mathscr{H}\left\{1 - \frac{V_{p,n}}{V_{p,crit}}\right\}, \tag{1}$$

where $\mathscr{H}\{x\}$ is the so-called Heaviside (unit) step function, with the following property:

$$\mathscr{H}\{x\} = \begin{cases} 1, & x \geqslant 0, \\ 0, & x < 0. \end{cases} \tag{2}$$

The inertial impaction correlations we have used to calculate the normal component of the impacting velocity, $V_{p,n}$ $(= V_p \cos\{\theta_i\})$ at each point on the upwind facing surface of a circular cylinder target in crossflow will be discussed in Section 2.3. The size dependence of the impacting particle critical velocity has been taken to be

$$V_{p,cr}\{v\} = V_{p,cr}\{v_{cr}\} \cdot (v/v_{cr})^{-1/2} = V_{p,cr}\{v_{cr}\} \cdot \xi^{-1/2} \tag{3}$$

although empirical exponents different from $-\frac{1}{2}$ are readily incorporated into such calculations (Wang and John, 1988). Wall *et al.* (1990) report critical velocity as a function of particle size for various combinations of projectile and target materials. Here v_{cr} is the volume of a particle of smallest size capable of inertially impacting in the prevailing environment calculated using methods discussed in Section 2.3. Our choice of exponent $-\frac{1}{2}$ to describe the size dependence of impacting particle critical velocity seems to be a reasonable one, based on results presented in Wall *et al.* (1990). We present our results (Section 3) in terms of the specifiable dimensionless "rebound parameter" $U/V_{p,cr}\{v_{cr}\}$,

where U is the mainstream velocity.[‡] In this scheme, the asymptotic limit $U/V_{p,cr}\{v_{cr}\} = 0$ corresponds to a sticking probability of unity irrespective of impact velocity. More complex dependencies on angle of incidence (see e.g. Xu *et al.*, 1993; Wang and John, 1988) and alternate $V_{p,cr}\{v\}$-dependencies will be considered in extensions of the present paper.

Incident particle capture by a 'granular' deposit. Recently, the sticking behavior of impacting particles on a dry "granular" deposit has been studied by Konstandopoulos (1991) and Rosner *et al.* (1992) using particle-level micromechanical computer simulation techniques. This important but complex case is still not fully understood, but we can already illustrate some of its distinguishing characteristics by invoking a sticking probability law based on these preliminary dynamical simulations. For the case of mono-sized particles impacting on a dry granular deposit, the relevant parameter is apparently the absolute impact velocity V_p (and not its normal component). If the impact velocity, V_p, is less than some critical velocity, the impacting particle is inevitably captured. But above this particle critical velocity, the sticking probability does not fall abruptly to zero; rather, it exhibits an exponential "tail" (see Fig. 2). Based on the abovementioned computer simulations, the

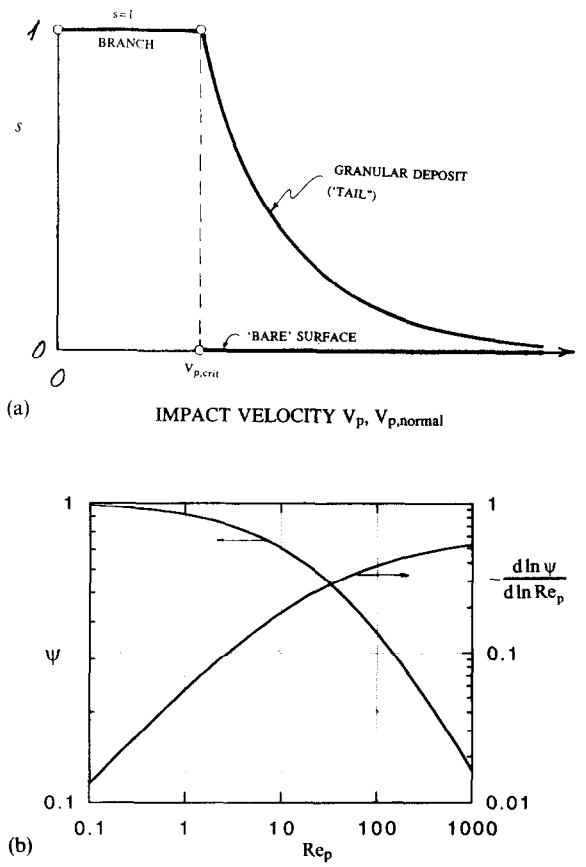

Fig. 2. (a) Single particle capture probability laws (particle velocity dependence). Cases shown: capture on a clean solid surface, and incipient capture by a granular deposit. (b) Non-Stokesian correction factor ψ for calculating effective Stokes number at characteristic particle Reynolds number Re_p (log–log).

[‡] A typical value of $U/V_{cr}\{v_{cr}\}$ is 9.5, for a polystyrene latex particle of critical size 5 μm impacting on a stainless steel target and mainstream velocity of 5 m s^{-1} (Cheng and Yeh, 1979).

sticking probability, s, for impacting particles on dry granular deposit is therefore tentatively approximated as follows:

$$s = \begin{cases} 1 & \text{for } V_p \leqslant V_{p,cr}\{v\}, \\ \exp\left\{-\chi_n \Theta\{\theta_i\} \cdot \left(\dfrac{V_p}{V_{p,crit}\{v\}} - 1\right)\right\} & \text{for } V_p \geqslant V_{p,cr}\{v\}. \end{cases} \tag{4}$$

The parameter χ_n defines the sensitivity of sticking probability to incident particle velocity when the particle velocity is greater than the critical velocity and directed normal to the target. The indicated function Θ defines the (comparatively weak) dependence of capture fraction on incidence angle (with respect to the underlying target) of the impacting particle. We neglect the particle size dependence of χ_n and the dependence of particle critical velocity on impingement angle, based again on the available (if not yet comprehensive) dynamical simulations of Konstandopoulos (1991). Therefore, for our illustrative particle-on-deposit simulations we choose the following relations for the parameters χ_n and Θ:

$$\begin{aligned} &\Theta = 1 + 0.2 \cdot \theta_i \quad (\theta_i \text{ in radians}) \\ &\chi_n = 0.8 \end{aligned} \tag{5}$$

As in the case of impaction on a clean smooth solid surface, we assume that $V_{p,cr}$ for impaction on a granular deposit is insensitive to angle of incidence and has the particle size dependence of equation (3)—a dependence which should be regarded as provisional—i.e. used here only for illustration purposes in the absence of definitive evidence to the contrary.

While, undoubtedly, the particular laws and parameter choices in equation (5) will have to be generalized, our "granular deposit" $(PSD)_W$ results below should be viewed as representative of what will happen when the single particle capture behavior does not depend only on the normal component of the velocity and has a non zero "tail" at impact velocities above some $V_{p,cr}$ (see Fig. 2a) (expected to be much smaller for impact on deposits compared to impact on hard solid surfaces and insensitive to incidence angles).

Resuspension (or erosion) of particles in the deposit caused by subsequent impinging particles will be neglected in the analysis which follows. Despite recent work on resuspension (John *et al.*, 1991; John and Sethi, 1993), a self-consistent theory (which can predict erosion yields for particles of different sizes, velocity and angle of incidence impacts on granular deposits) is not available.[§] We are now developing particle-level micromechanical models for estimating erosion yield laws for impaction on a granular deposit, and these results will be incorporated in extensions of this work.

2.3. *Inertial impaction for a cylindrical target in crossflow*; Stk_{eff} *correlations*

Defined as the ratio of the characteristic *stopping time* $t_p (= \tilde{\rho}_p d_p^2/18\mu)$ to the *flow time* t_{flow} $(\equiv (d_t/2)/U)$ the *Stokes number*, Stk, which dictates particle impaction behavior in any aerodynamic environment, is conventionally computed assuming the linear Stokes drag law (see e.g. Friedlander (1977) or Rosner (1986)). In an analysis of inertial impaction on spheres and circular cylinders in high-speed streams Israel and Rosner (1983) introduced a *generalized Stokes number*, Stk_{eff}, which takes into account the non-Stokesian drag on the particles and possible systematic modifications of t_{flow} (e.g. due to the adjacent targets; see e.g. Konstandopoulos *et al.*, 1993). It may be calculated in terms of conventionally defined Stokes number and particle Reynolds number (Re_p) via

$$Stk_{eff} = Stk \cdot \psi\{Re_p\}. \tag{6}$$

[§] Crude approximations have been made to estimate deposit erosion yield behavior by treating the deposit to be 'semi-ductile' (with erosion behavior qualitatively similar to that of metals) (see e.g. Miller *et al.*, 1992). Although we are interested in the erosion of *deposits* by impacting particles, as a first step towards that goal, we have developed a rational, convenient method to predict solid target cylinder erosion rates for metals (Rosner *et al.*, 1995; Kho *et al.*, 1995) and ceramics (Khalil and Rosner, 1995) when erosion yield data are available.

The non-Stokes drag correction factor, $\psi\{\mathrm{Re_p}\}$, can be calculated from (Israel and Rosner, 1983):

$$\psi\{\mathrm{Re_p}\} = \frac{24}{\mathrm{Re_p}} \int_0^{\mathrm{Re_p}} \frac{\mathrm{d\,Re'}}{C_D\{\mathrm{Re'}\}\,\mathrm{Re'}} \tag{7}$$

and is seen to have the necessary property $\psi \to 1$ when the drag coefficient $C_D \to 24/\mathrm{Re}$ (Stokesian limit). A useful empirical approximation to extensive $C_D\{\mathrm{Re}\}$ data, accurate up to $\mathrm{Re_p} = O\{10^3\}$, is

$$C_D \cong \frac{24}{\mathrm{Re}}[1 + 0.158\ (\mathrm{Re})^{2/3}]. \tag{8}$$

This representation leads to a correction factor ψ which can be explicitly expressed in terms of $\mathrm{Re_p}$ as

$$\psi = \frac{3\{\sqrt{c}\,\mathrm{Re_p^{1/3}} - \tan^{-1}\{\sqrt{c}\,\mathrm{Re_p^{1/3}}\}\}}{c^{3/2}\,\mathrm{Re_p}}. \tag{9}$$

This convenient relation, with $c = 0.158$, has been used for all $(\mathrm{PSD})_w$ calculations reported here, as well as the construction of Fig. 2b (with log–log coordinates). The integrations over particle volume required to calculate the particle size distribution in the deposit will be carried out using the dimensionless particle volume variable $\xi \equiv v/v_{cr}$. However, all inertial impaction correlations (Israel and Rosner, 1983; Wang, 1986; Wessel and Righi, 1988; Konstandopoulos *et al.*, 1993) are given in Table 1 in terms of the *effective Stokes number* of equation (6), or explicitly

$$\mathrm{Stk_{eff}} \equiv \mathrm{Stk} \cdot \psi\{Ud_p/\nu\} = \frac{1}{9}\frac{\tilde{\rho}_p U d_p^2}{\mu_g d_t} \cdot \psi\{Ud_p/\nu\}. \tag{10}$$

When use is made of the result that the singular size v_{cr} ($\equiv \pi d_{p,cr}^3/6$) corresponds to $\mathrm{Stk_{eff,cr}} = \frac{1}{8}$ (for a circular cylinder target at $\mathrm{Re_t^{1/2}} \gg 1$) the algebraic (transcendental)[¶] relation between the variables $\mathrm{Stk_{eff}}$ and ξ is easily seen to be obtainable from (using equations (9) and (10)):

$$\mathrm{Stk_{eff}} = \frac{1}{8}\xi^{1/3} \cdot \left\{\frac{\sqrt{c}\,\mathrm{Re_{p,cr}^{1/3}}\xi^{1/9} - \tan^{-1}\{\sqrt{c}\,\mathrm{Re_{p,cr}^{1/3}}\xi^{1/9}\}}{\sqrt{c}\,\mathrm{Re_{p,cr}^{1/3}} - \tan^{-1}\{\sqrt{c}\,\mathrm{Re_{p,cr}^{1/3}}\}}\right\} \tag{11}$$

where $\mathrm{Re_{p,cr}}$, the value of $Ud_{p,cr}/\nu_g$ (of the order unity for many cases of present interest), will remain as an important parameter in all of the following calculations.

Table 1. Constants in correlation equations 12 and 13 for estimating particle local impingement velocity, angle and dimensionless collision frequency (after Wessel and Righi (1988))

Correlation parameter, Γ	Correlation constants				Correlation equation
	$\mathrm{Stk_{eff}}$ range	β_1	β_2	β_3	
Target efficiency, η_{cap}	$0.125 \to 0.5$	0.01978749	0.5136545	−0.0482858	equation 12
	> 0.5	1.54424	−0.538313	0.2020116	equation 13
Maximum angle experiencing impingement, $\theta_m/(\pi/2)$	$0.125 \to 0.5$	0.696596	−1.822407	1.1452745	equation 12
	> 0.5	0.7722744	−0.271871	0.06049905	equation 13
Impact velocity, $\lvert V_p\{0\}\rvert/U$	$0.125 \to 0.8$	0.0209863	0.8762208	−0.403482	equation 12
	> 0.8	1.038627	−0.327754	0.1115756	equation 13
Impact velocity, $\lvert V_p\{\theta_m\}\rvert/U$	$0.125 \to 0.5$	1.925045	−6.38525	3.796702	equation 12
	> 0.5	−0.242589	0.234317	−0.0446577	equation 13

[¶] If it were not for the non-Stokesian correction $\psi\{\mathrm{Re_p}\}$, $\mathrm{Stk_{eff}}$ for particles large enough to remain in the continuum regime would simply be proportional to $\xi^{2/3}$ (i.e. projectile particle surface area).

For a circular cylinder target in crossflow, the basic inertial impaction functions: overall impingement efficiency (η_{cap}), the maximum angle of experiencing impingement (θ_{max}), the impact speeds at the forward stagnation point (V_{p0}) and at the maximum angle experiencing impingement (V_{pm}) have been recalculated via numerical integration of the particle trajectory equations and the results are correlated by Wessel and Righi (1988) (W&R) henceforth using the notion of an effective Stokes number, Stk_{eff}, recommended by Israel and Rosner (1983). The correlation forms used are

$$\Gamma = \beta_1 \ln(8Stk_{eff}) + \beta_2 (Stk_{eff} - \tfrac{1}{8}) + \beta_3 (Stk_{eff} - \tfrac{1}{8})^2 \tag{12}$$

or (cf. Israel and Rosner, 1983)

$$\Gamma = \{1 + \beta_1 (Stk_{eff} - \tfrac{1}{8})^{-1} + \beta_2 (Stk_{eff} - \tfrac{1}{8})^{-2} + \beta_3 (Stk_{eff} - \tfrac{1}{8})^{-3}\}^{-1}, \tag{13}$$

where the recommended values for the coefficients appearing in these formulae are reproduced in Table 1. In addition, Wessel and Righi (1988) provide a set of correlations for "local" normalized impingement efficiency ($\eta_{loc}\{\theta\}$; cf. Section 2.3) at any angular position, θ, in terms of the overall impingement efficiency (η_{cap}) and the maximum angle, θ_{max}, experiencing impingement (θ_{max}).

$$\eta_{loc}\{\theta\} = \frac{\pi}{2}\frac{\eta_{cap}}{\theta_{max}} \cdot \cos\left\{\frac{\pi}{2}\frac{\theta}{\theta_{max}}\right\}. \tag{14}$$

The impact speed ($V_p\{\theta\}$) of a particle at any point ($\theta \leqslant \theta_{max}$) on the surface is correlated with the above mentioned values V_{pm}, V_{p0} and θ_{max} via

$$V_p\{\theta\} = -(V_{pm} - V_{p0}) \cdot \cos\left(\frac{\pi}{2}\frac{\theta}{\theta_{max}}\right) + V_{pm}. \tag{15}$$

The complement ($\alpha\{\theta\}$) of the angle of incidence θ_i (Fig. 1)) depends on the maximum angle experiencing impaction and an exponent, b, also correlated with Stk_{eff} via

$$\frac{\alpha\{\theta\}}{(\pi/2)} = \left\{1 - \left(\frac{\theta}{\theta_{max}}\right)^{1/b}\right\}^b, \tag{16}$$

where

$$b = 1 + \frac{\beta_1}{Stk_{eff}} + \frac{\beta_2}{Stk_{eff}^2} + \frac{\beta_3}{Stk_{eff}^3} \tag{17}$$

and, according to Wessel and Righi (1988) $\beta_1 = 0.1851488$, $\beta_2 = -0.0205901$ and $\beta_3 = 0.001530146$. Thus, in our present notation $h \equiv \theta_i/(\pi/2) = 1 - [\alpha\{\theta\}/(\pi/2)]$. In closing this section we note that compact alternative correlations for η_{cap} and $V_p\{\theta\}/U$ have also been provided by Wang (1986), however we have chosen not to "mix" correlations from different sources.

The correlations defined above for functions η_{loc}, V_p and θ_i have been described in terms of effective particle Stokes number, which can be calculated for a particle of given size using equation (11). These functions are used in evaluating particle size distribution in the deposit (equations (20) and (21)–Section 2.5). The capture fraction, s, appearing in these equations depends on the impingment velocity V_p and impinging angle θ_i, both of which are themselves function of impacting particle size v and position θ on the upwind side of the circular cylinder.

2.4. *Particle size distribution in the mainstream*

Using particle volume $v(=\pi d_p^3/6$ for a sphere of diameter d_p) as the basic size variable, the normalized mainstream distribution function $C_\infty\{v\}$ appearing in Section 2.3 is defined such that the mainstream number density of particles with volume $v \pm (dv/2)$ is given by $N_p C_\infty\{v\} \cdot dv$, where N_p is the total particle number density. While the quadrature expressions given below for the normalized distribution function $C_{dep}\{v\}$ (Section 2.5) admit *any*

$C_\infty\{v\}$ of particular interest, all of the remaining calculations here will be based on the single-mode, two-parameter continuous distribution function in the mainstream:

$$C_\infty\{v\} = \frac{1}{v\sqrt{2\pi}\ln\sigma_g} \cdot \exp\left[-\frac{(\ln\{v/v_g\})^2}{2\ln^2\sigma_g}\right], \tag{18}$$

which is said to be "log-normal" since $v \cdot C_\infty\{v\}$ is Gaussian in the particle volume variable $\ln v$. A particular value of the spread parameter of special interest here is $\sigma_g = 2.3$, corresponding closely to coagulation-aged populations in the continuum regime (see e.g. Friedlander, 1977; Rosner and Tassopoulos, 1989)). Rather than using the geometric mean particle volume v_g to characterize the average particle size in the population, we choose instead the number-mean volume defined by the integral of $vC_\infty\{v\}$ over all particle sizes in the mainstream population, where, for a log-normal population (see e.g. Rosner and Tassopoulos, 1991):

$$\bar{v} = v_g \exp\{\ln^2\sigma_g/2\}. \tag{19}$$

As noted earlier, the product $\bar{v} \cdot N_p$ is the total *volume fraction* $\phi_{p,\infty}$ of the mainstream aerosol, assumed here to be a very small number ($\ll 1$).

2.5. *Local size distribution of captured particles*

For the log-normal distribution C_∞ (equation (18)) and the single particle capture probability law $s\{v, \theta\}$ (Section 2.2) calculated in terms of local impingement velocity, angle and dimensionless collision frequency (Section 2.3), we calculate below the *deposit* local particle size distribution from the normalized quadrature expression:

$$C_{dep}\{v, \theta\} = \frac{\{s\{v, \theta\}\eta_{loc}\{v, \theta\}C_\infty\{v\}\}}{\int_0^\infty s\{v, \theta\}\eta_{loc}\{v, \theta\}C_\infty\{v\}dv}. \tag{20}$$

The sticking coefficient, s, and the dimensionless local impingement frequency, η_{loc}, at each position θ and particle size v are evaluated using the relation between effective Stokes number, Stk_{eff}, and dimensionless particle volume, $\xi\ (\equiv v/v_{cr})$ (equation (11)), where v_{cr} is the critical volume, i.e. the volume of the smallest particle capable of inertial impaction on the target in the prevailing environment, and $Re_{p,cr}$, the Reynolds number based on mainstream velocity and diameter of critical size particle. The above integral can easily be calculated and reported in the equivalent nondimensional form:

$$C_{dep}\{\xi, \theta\}v_{crit} = \frac{\{s\{\xi, \theta\}\eta_{loc}\{\xi, \theta\}C_\infty\{\xi\}\}}{\int_0^\infty s\{\xi, \theta\}\eta_{loc}\{\xi, \theta\}C_\infty\{\xi\}d\xi}. \tag{21}$$

We present our results as the normalized deposit particle size distribution $C_{dep}v_{cr}$ at different "sampling" positions θ on the upwind surface of the circular cylinder for each of the single particle sticking laws discussed in Section 2.2. For the cases where $(PSD)_w$ can itself be approximated by a log-normal distribution we also report the standard deviation, $\sigma_{g,dep}$ and number mean $\bar{\xi}_{dep}$, of the *deposit* particle size distribution $(PSD)_w$.

In some applications, all deposit particle populations on the *upwind* target surface may be 'pooled',[‖] in which case one would obtain a size distribution $\bar{C}_{dep}\{v\}$ which is a suitably weighted combination of the above mentioned local distribution functions $C_{dep}\{v, \theta\}$. In such cases, we expect

$$\bar{C}_{dep}\{v\} = \frac{2}{\pi} \cdot \int_0^{\pi/2} F\{\theta\} \cdot C_{dep}\{v, \theta\}d\theta, \tag{22}$$

where, from equation (20), the indicated "weighting" function $F\{\theta\}$ can be expressed as

$$F\{\theta\} = f\{\theta\}/\bar{f} \tag{23}$$

[‖] As, for example, if the target undergoes continuous *rotation* such that $\Omega d_t/2 \ll U$.

in terms of the target position-dependent integral over all particle sizes:

$$f\{\theta\} \equiv \int_0^\infty s\{v, \theta\} \cdot \eta_{\text{loc}}\{v, \theta\} \cdot C_\infty\{v\} \mathrm{d}v \tag{24}$$

and its upwind surface average:

$$\bar{f} \equiv \frac{2}{\pi} \cdot \int_0^{\pi/2} f\{\theta\} \mathrm{d}\theta. \tag{25}$$

Typical results for this "upwind-pooled" $(\text{PSD})_w$ will also be included in Section 3, at least for the case $s = \text{const}$. We notice that the interpretation of such pooled data will inevitably be compromised by the loss of information associated with spatial averaging. Moreover, since a cylindrical target lends itself (via physical rotation of the active sampling "sector") to angle-dependent PSD_w-information, we recommend that this feature be *exploited* to confirm one's understanding of the nature of the mainstream population $C_\infty\{v\}$ and the operative capture law $s\{V_p\{v, \theta\}/U; \theta_i\{v, \theta\}\}$.

3. RESULTS AND DISCUSSION

3.1. *Deposit particle size distribution*

For the log-normal distribution C_∞ and the single particle capture laws, local impingement angle and efficiencies discussed in Section 2, we have calculated the normalized deposit local size distribution ($(\text{PSD})_w$) at different positions on the upwind surface of a circular cylinder using equation (21). The *spread* of the local particle size distribution in the deposit is often quite different from the spread of the particle log-normal size distribution in the mainstream and, for most cases $(\text{PSD})_w$ cannot be accurately represented by an approximate log-normal distribution function. However, for those cases where $(\text{PSD})_w$ *can* be represented as a log-normal distribution, we calculate (using methods discussed in Raabe (1971)) and report the geometric standard deviation, $\sigma_{g,\text{dep}}$. The mean dimensionless particle size in the deposit reported in Fig. 7 can be used to calculate the median particle size for the deposit log-normal distribution using

$$\xi_{g,\text{dep}} = \bar{\xi}_{\text{dep}} \cdot \exp\{-\tfrac{1}{2}\ln^2\sigma_{g,\text{dep}}\}. \tag{26}$$

In Figs 3–6, we show the computed normalized $(\text{PSD})_w$ for different sticking laws (H in these figures corresponds to the Heaviside-type sticking law (equations (1) and (2)) describing sticking behavior on smooth ("bare") solid surfaces while the abbreviation "Gr" refers to the sticking behavior on a granular deposit; (equation (4)) at different positions on the upwind surface of the circular cylinder in crossflow for a log-normal mainstream particle size distribution. We report here our results for a mainstream standard deviation, σ_g, of 2.3, i.e. the "self-preserving" spread corresponding to coagulation-aged populations in the continuum regime (see e.g. Rosner and Tassopoulos, 1989).

3.2. *Constant capture fraction*

For the case of impact-velocity independent constant sticking law (here labeled $s = 1$), when the mean dimensionless particle size in the mainstream, $\bar{\xi}$, is small, a major fraction of the particles fall in the subcritical range and do not deposit by mechanism of inertial impaction. Therefore, for such cases, particles from only the large size "tail" of the distribution in the mainstream are able to deposit, leading to a deposit size distribution very different from log-normal. As the mean dimensionless size, $\bar{\xi}_\infty$, in the mainstream increases, a smaller and smaller fraction of particles lie in the subcritical range incapable of impacting the target, so that, for large values of mean particle size in the mainstream the deposit distributions are very close to log-normal distributions. The spreads of these populations

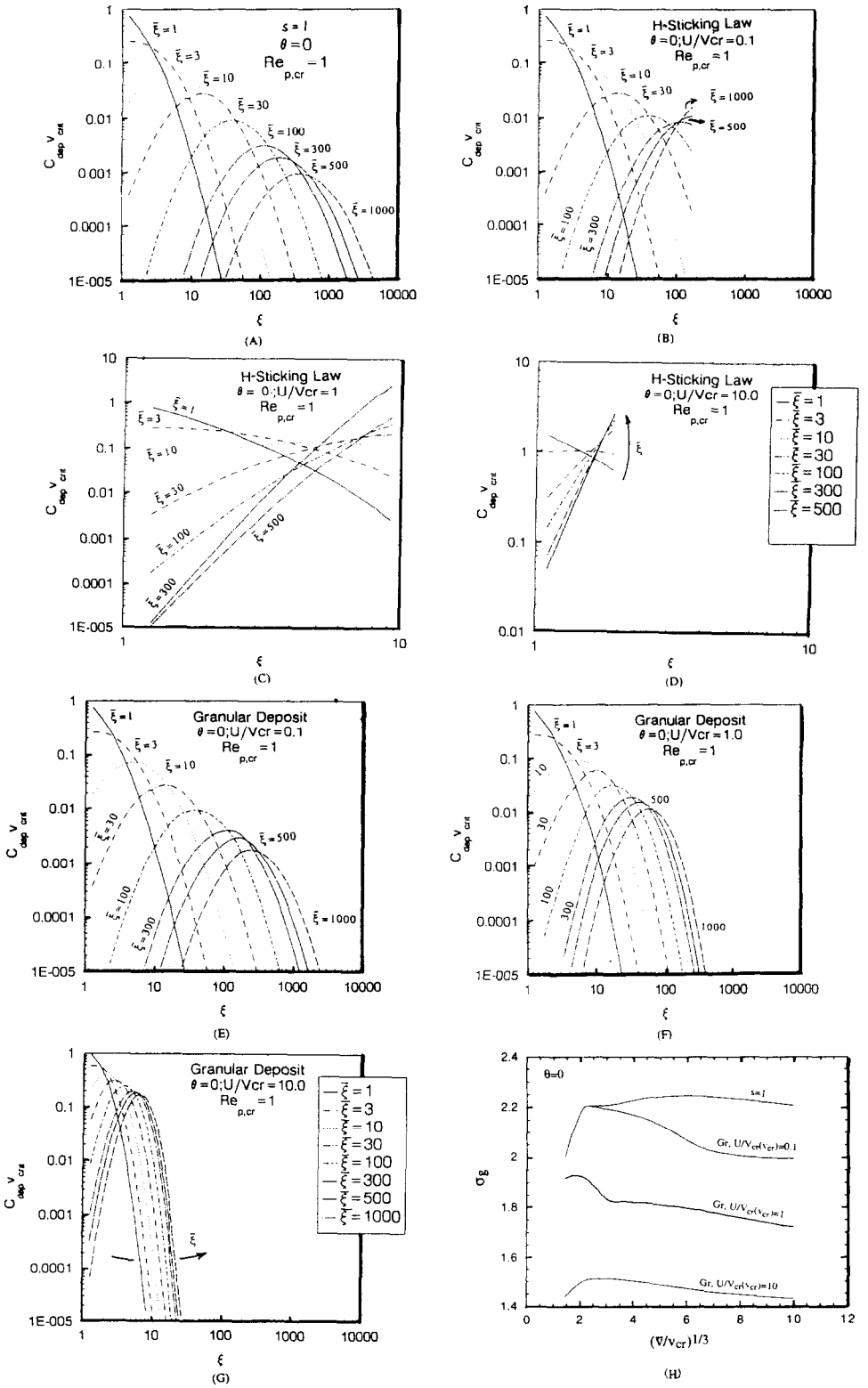

Fig. 3. Local particle size distribution in deposit at angular position $\theta = 0$. Cases shown: (A) $s = 1$; (B) impaction on clean smooth surface with $U/V_{cr}(v_{cr}) = 0.1$; (C) impaction on clean smooth surface with $U/V_{cr}(v_{cr}) = 1.0$; (D) impaction on clean smooth surface with $U/V_{cr}(v_{cr}) = 10$; (E) impaction on granular deposit with $U/V_{cr}(v_{cr}) = 0.1$; (F) impaction on granular deposit with $U/V_{cr}(v_{cr}) = 1.0$; (G) impaction on granular deposit with $U/V_{cr}(v_{cr}) = 10$. In (H) we show the spreads of the deposit particle size distribution for cases when these are approximate log-normal.

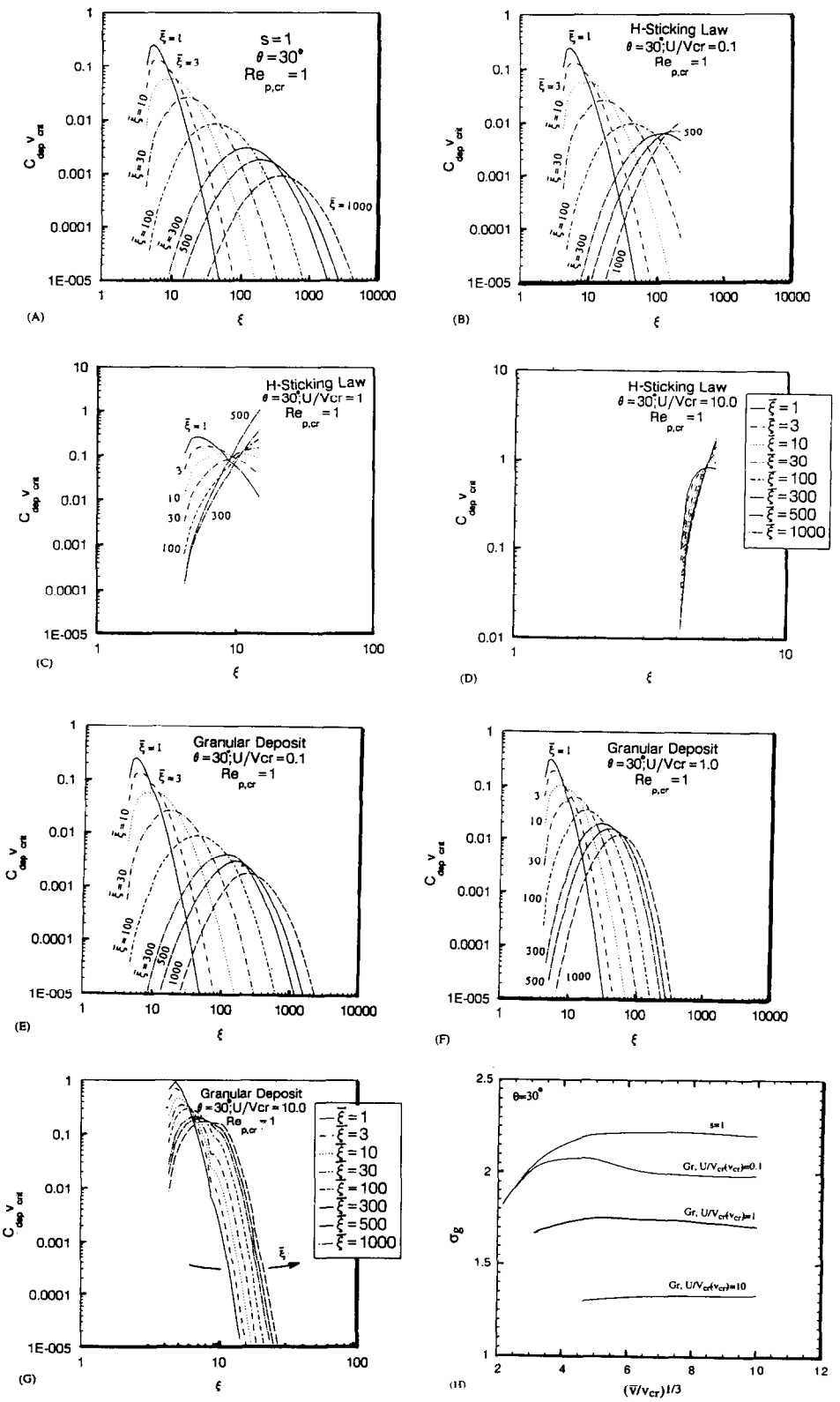

Fig. 4. Local particle size distribution in deposit at angular position $\theta = 30°$. Cases shown: (A) $s = 1$; (B) impaction on clean smooth surface with $U/V_{cr}(v_{cr}) = 0.1$; (C) impaction on clean smooth surface with $U/V_{cr}(v_{cr}) = 1.0$; (D) impaction on clean smooth surface with $U/V_{cr}(v_{cr}) = 10$; (E) impaction on granular deposit with $U/V_{cr}(v_{cr}) = 0.1$; (F) impaction on granular deposit with $U/V_{cr}(v_{cr}) = 1.0$; (G) impaction on granular deposit with $U/V_{cr}(v_{cr}) = 10$. In (H) we show the spreads of the deposit particle size distribution for cases when these are approximate log-normal.

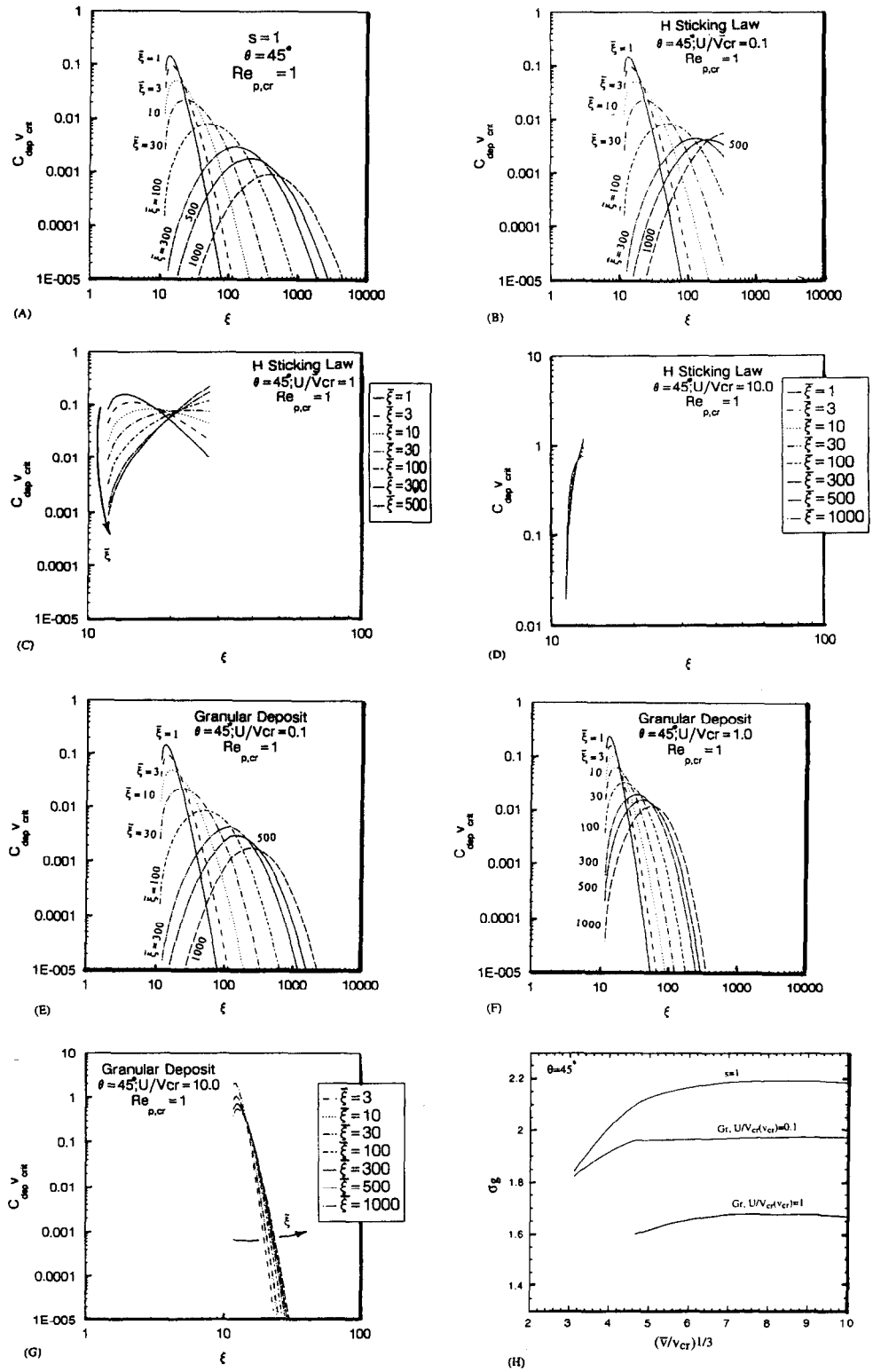

Fig. 5. Local particle size distribution in deposit at angular position $\theta = 45°$. Cases shown: (A) $s = 1$; (B) impaction on clean smooth surface with $U/V_{cr}(v_{cr}) = 0.1$; (C) impaction on clean smooth surface with $U/V_{cr}(v_{cr}) = 1.0$; (D) impaction on clean smooth surface with $U/V_{cr}(v_{cr}) = 10$; (E) impaction on granular deposit with $U/V_{cr}(v_{cr}) = 0.1$; (F) impaction on granular deposit with $U/V_{cr}(v_{cr}) = 1.0$; (G) impaction on granular deposit with $U/V_{cr}(v_{cr}) = 10$. In (H) we show the spreads of the deposit particle size distribution for cases when these are approximate log-normal.

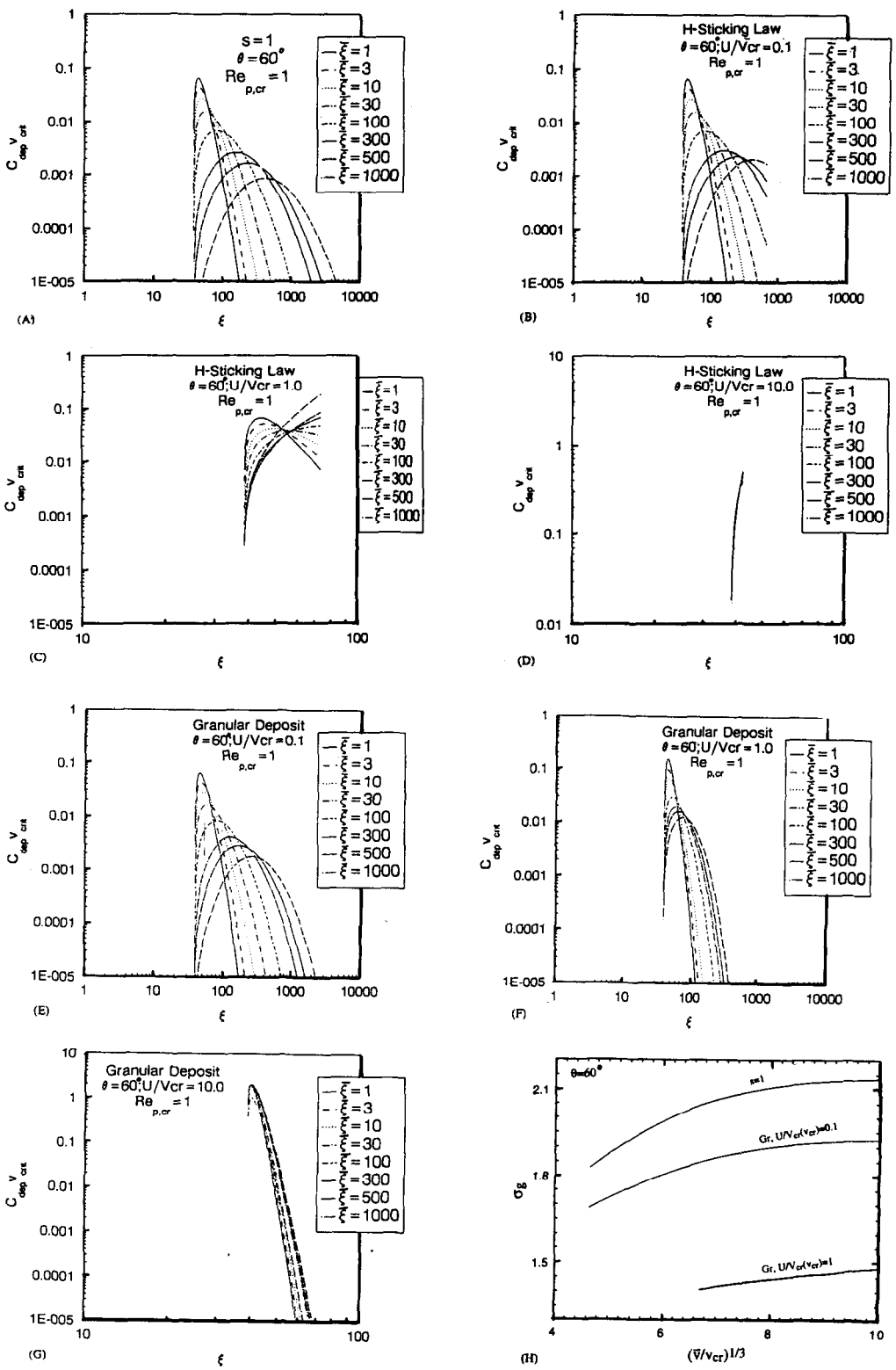

Fig. 6. Local particle size distribution in deposit at angular position $\theta = 60°$. Cases shown: (A) $s = 1$; (B) impaction on clean smooth surface with $U/V_{cr}(v_{cr}) = 0.1$; (C) impaction on clean smooth surface with $U/V_{cr}(v_{cr}) = 1.0$; (D) impaction on clean smooth surface with $U/V_{cr}(v_{cr}) = 10$; (E) impaction on granular deposit with $U/V_{cr}(v_{cr}) = 1.0$; (F) impaction on granular deposit with $U/V_{cr}(v_{cr}) = 1.0$; (G) impaction on granular deposit with $U/V_{cr}(v_{cr}) = 10$. In (H) we show the spreads of the deposit particle size distribution for cases when these are approximate log-normal.

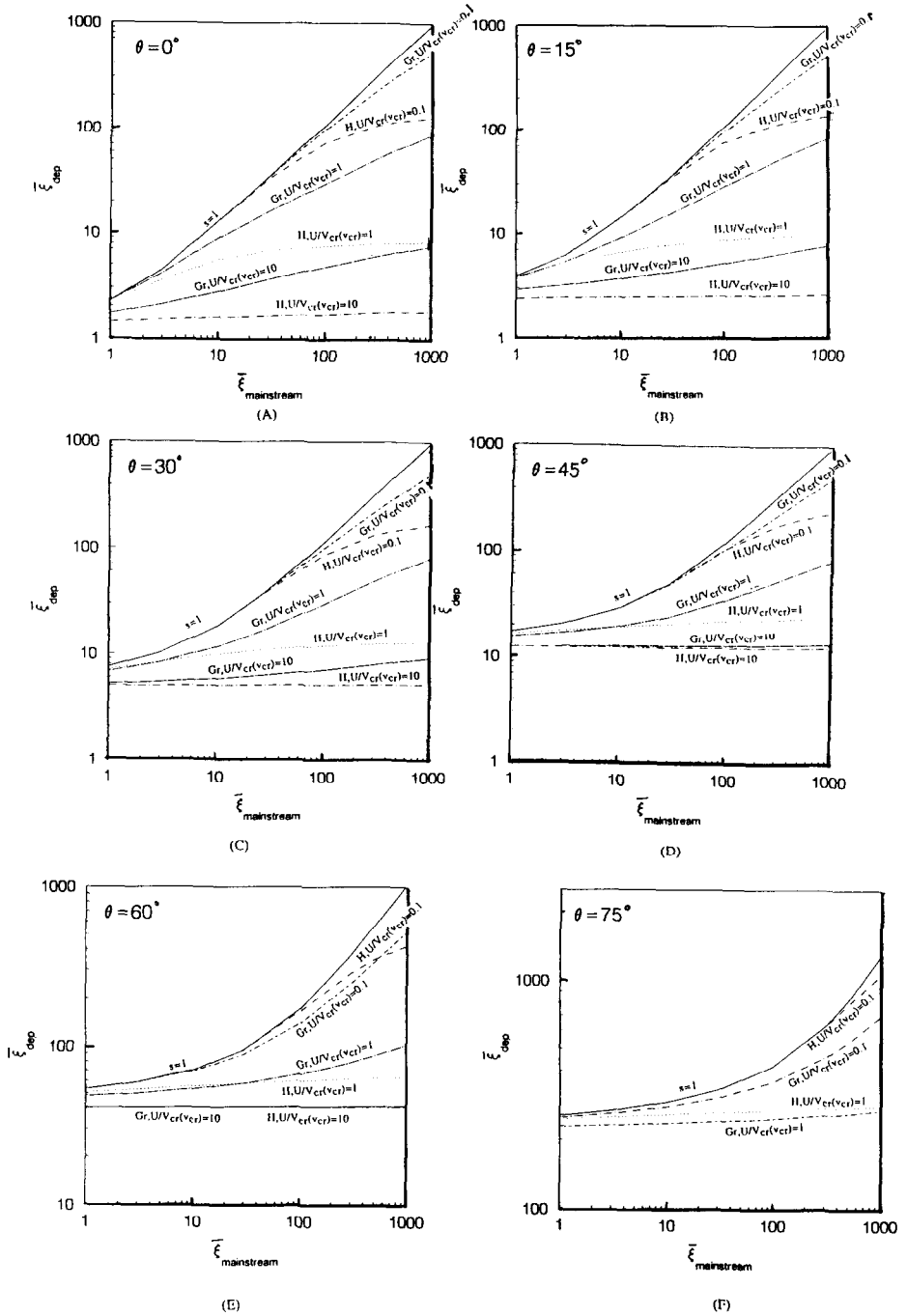

Fig. 7. Mean particle size in the deposit as a function of mean particle size in the mainstream for different positions. Cases shown (A) $\theta = 0°$; (B) $\theta = 15°$; (C) $\theta = 30°$; (D) $\theta = 45°$; (E) $\theta = 60°$; (F) $\theta = 75°$ (H—Heaviside sticking law; Gr—impaction on granular deposit).

are not very different from the spread in the mainstream ($\sigma_g = 2.3$). However, the mean particle size of these distributions starts higher than the mean volume in the mainstream but approach the mainstream value for high mean particle size in the mainstream (Fig. 7).

It is interesting and instructive to compare these results with the earlier conclusions of Rosner and Tassopoulos (1989, 1991), and Rosner (1989) for the special case of "power-law

capture" from a log-normal mainstream distribution—i.e. particle deposition under conditions where rebound is not a factor (say $s=1$) and $b \equiv \partial \ln \mathrm{St_m}/\partial \ln v = \text{const}$, where $\mathrm{St_m}$ is the mass transfer (Stanton) coefficient (Rosner, 1986, 1989). In that case the spread $\sigma_{g,dep}$ of the particle population in the deposit is exactly the same as the particle spread σ_g in the mainstream, but the mean particle volume (v_g or $\bar{v}$) in the deposit is systematically shifted by the ratio (Rosner and Tassopoulos, 1991)

$$\frac{\bar{v}_{dep}}{\bar{v}} = \exp\left[\frac{b}{2}\cdot \ln^2\{\sigma_g\}\right], \tag{27}$$

which differs from unity whenever the exponent b is nonzero—i.e. when $\mathrm{St_m}$ is particle size dependent. Thus, if (for Brownian diffusion of dense spherical particles across an isothermal turbulent boundary level at $\mathrm{Sc} \gg 1$) $b = -0.235$ (Rosner and Tassopoulos, 1989) the mean particle size in the deposit will be less than in the mainstream by the factor 0.922 (when $\sigma_g = 2.3$) since the capture of larger particles is less efficient. In the absence of rebound phenomena, inertially modified particle deposition leads to positive values of the exponent b (i.e. larger particle capture is favored) and we expect that the mean particle volume in such deposits would exceed that in the mainstream—e.g. for "eddy impaction" with $b = +1.333$ (Rosner and Tassopoulos, 1989) we find $\bar{v}_{dep}/\bar{v} = 1.59$. For the presently considered case of *inertial impaction on a circular cylinder in crossflow, there is no single value of the exponent* b applicable over the supercritical size range of interest (Rosner and Tassopoulos, 1989) so that equation (27) is not applicable to the deposited population(s).

3.3. *Capture on clean solid surfaces*

For the simplest case of impingement on clean solid surfaces, a particle is captured only if its normal velocity component, $v_{p,n}$, is less than some size-dependent critical velocity,** $V_{p,cr}\{v\}$. Therefore, the deposit only contains particles from the small size, yet supercritical portion of the mainstream distribution. As the mean particle size in the mainstream increases, only an insignificant fraction of these particles are in the sub-critical region resulting in approximate log-normal $(\mathrm{PSD})_w$. With further increase in the mean particle size in the mainstream, a larger fraction of these particles rebound upon impaction on the surface (Fig. 8), resulting in particles captured from the small size end (which is supercritical) of the mainstream log-normal distribution. As the rebound parameter (ratio of the mainstream velocity U to the threshold critical velocity, $V_{p,cr}\{v_{cr}\}$ increases, a larger fraction of impacting particles rebound, leading to narrower distributions in the deposit.

When the mainstream velocity is very much larger than the threshold velocity for the particle capture/rebound transition (evaluated at the particle size corresponding to incipient impaction) then only slightly supercritical size particles can be captured, with the remainder of the impacting particles rebounding. This implies that, of all particles in the mainstream distribution, the target will only be able to capture a small "slice", corresponding the fraction:

$$\Phi_{stick} = \frac{1}{\bar{v}}\cdot \int_{v_{cr}}^{v_{reb}} v\, C_\infty\{v\}\, dv \tag{28}$$

of the total population (i.e. those particles capable of impacting but not rebounding).†† Indeed, when v_{reb} is very close to v_{cr} this integral may be approximated by

$$\Phi_{stick} = v_{cr} C_\infty\{v_{cr}\}\cdot \frac{v_{cr}}{\bar{v}}\cdot \left\{3\left[\left(\frac{v_{reb}}{v_{cr}}\right)^{1/3} - 1\right]\right\}. \tag{29}$$

** More generally, the critical velocity is dependent on angle of incidence (Wang and John, 1988; Xu *et al.*, 1993). Such cases will be readily studied in our follow-on work.

†† In considering the "inverse" problem of constructing $C_\infty\{v\}$ from $C_{dep}\{v\}$-information (Section 5) it is clear that in such a case we will only be able to reconstruct at most this "slice" of $C_\infty\{v\}$ (see Fig. 10).

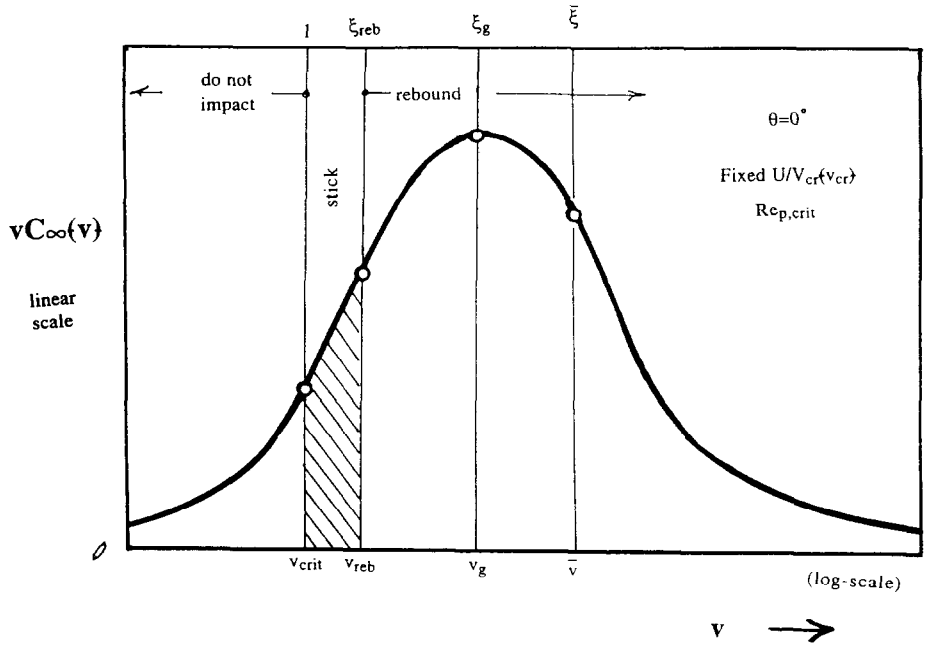

Fig. 8. Fraction of mainstream particle size distribution capable of impacting (stagnation point, $\theta = 0$) without rebounding; schematic showing nomenclature.

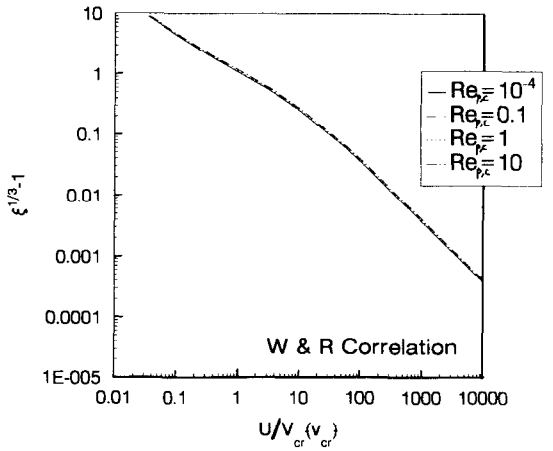

Fig. 9. Plot of $\xi_{reb}^{1/3} - 1$ (where $\xi_{reb} \equiv v_{reb}/v_{cr}$ is the dimensionless particle size for incipient rebound) vs the ratio of mainstream velocity to the critical velocity for rebound of a hypothetical impacting particle of critical size.

The behavior of $\xi_{reb}^{1/3} \equiv (v_{reb}/v_{cr})^{1/3}$ at very large values of rebound parameter $U/V_{p,cr}\{v_{cr}\}$ may be studied using, say, the impact velocity correlation of Wessel and Righi (1988). Our results for forward stagnation point are shown in Fig. 9 over a range of the non-Stokesian parameter Re_p, from 0 (Stokes drag) to 10. The corresponding behavior of Φ_{stick} is shown in Fig. 10 for a mainstream population spread of 2.3. Increasing the rebound parameter, $U/V_{cr}\{v_{cr}\}$, leads to a decrease in the mean particle size in the deposit (Fig. 7) as a larger fraction of particles rebound upon impact with the surface.

3.4. *Capture on granular deposit*

In the case of particle impaction on a granular deposit, a particle is still captured when its impact velocity, V_p, is less than some size-dependent critical velocity, however, above this

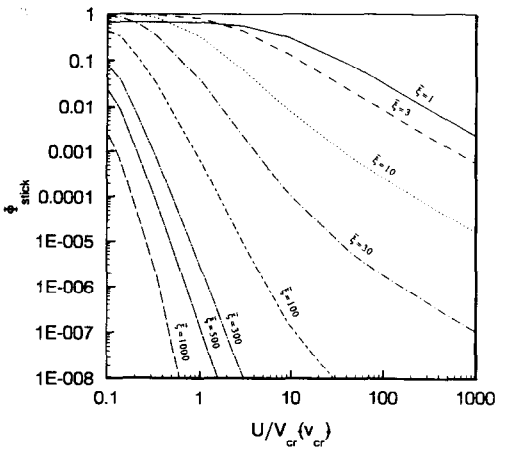

Fig. 10. Plot of fraction of mainstream particles capable of both impacting and sticking at forward stagnation point, as a function of the rebound parameter $U/V_{cr}\{v_{cr}\}$.

threshold velocity the capture fraction decays exponentially to zero (Section 2.2). As with the increase of mainstream mean particle size, beyond a certain velocity, a larger fraction of the mainstream particle population rebound from the granular surface, the spreads of the deposit particle population on such surfaces are much smaller than the mainstream population spread. As the rebound parameter increases, a larger fraction of the particles in the mainstream rebound from the surface, resulting in deposits with narrower spreads and *smaller* mean particle sizes.

3.5. *Position dependence*

For the case of sticking fraction law independent of both impact velocity and angle, the spread of $(PSD)_w$ decreases (Figs 3–6) while the mean particle size in the deposit increases (Fig. 7) at higher angular position, θ, because only a smaller fraction of particles are capable of inertially impacting there. Similarly, for the case of particle capture on clean-smooth and granular surfaces, when the mean particle size in the mainstream is small, particles which can be captured in the forward stagnation region are incapable of inertially impacting at higher angles. But, as the mean size in the mainstream increases, a larger fraction of these particles which rebound in the forward stagnation region are captured at larger angles. Thus, the size distribution at such locations is shifted toward larger size particles resulting in higher mean size particle (Fig. 7). While $(PSD)_w$-data at any location may lead to reconstruction of only a part of supercritical portion of $C_\infty\{v\}$ (Section 4), the complete $C_\infty\{v\}$ may be reconstructed with the help of $(PSD)_w$-data from other target locations on the same body (Fig. 11).

3.6. *"Pooled" deposit particle size distribution*

In log-log plot Fig. 12a we show some examples of out "pooled" $\bar{C}_{dep}\{v\}$ results for the simplest case of constant sticking fraction ($s = 1$), using the computational methods discussed in Section 2.5. Because such target does not "see" the subcritical size particles contained in $C_\infty\{v\}$, the mean particle sizes in such "pooled" populations, shown in Fig. 12b, are found to be systematically higher than the corresponding mainstream mean particle sizes. This is also shown in Fig. 12a, which superimposes $v_{cr}C_\infty\{\xi\}$ for the particular case $\bar{\xi}_\infty = 30$.

4. IMPLICATIONS AND APPLICATIONS

The local size distribution of particles in the deposit will usually be required in addition to the total rate of deposition (Rosner and Tandon, 1995; Tandon, 1995) to predict, say, the

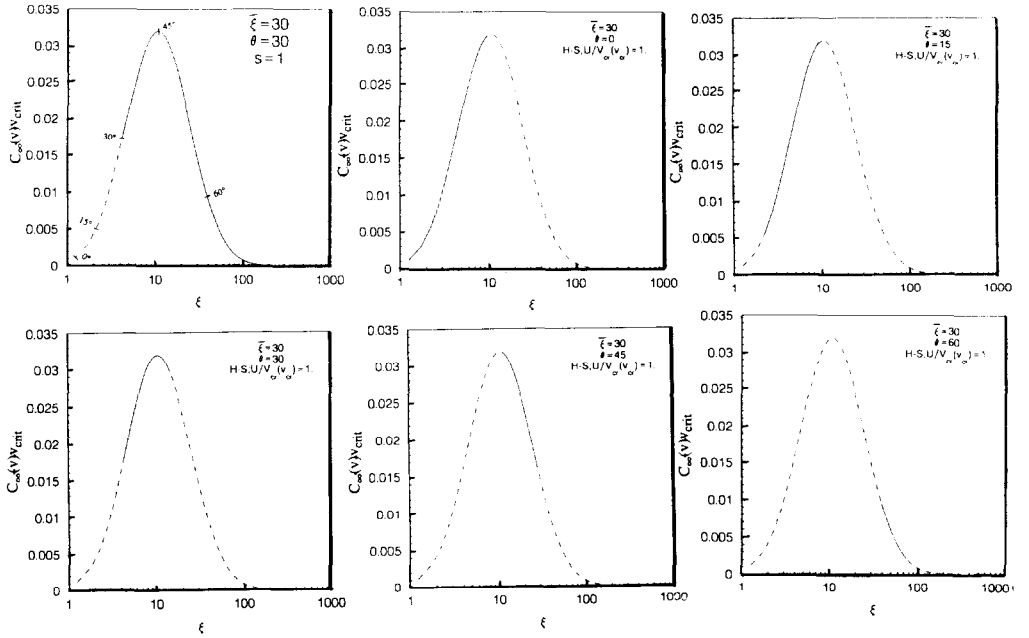

Fig. 11. Construction of $C_{\infty}\{v\}$ distribution from $C_{dep}\{v\}$ data (solid line: part of mainstream distribution that *can* be reconstructed; dotted line: actual mainstream distribution).

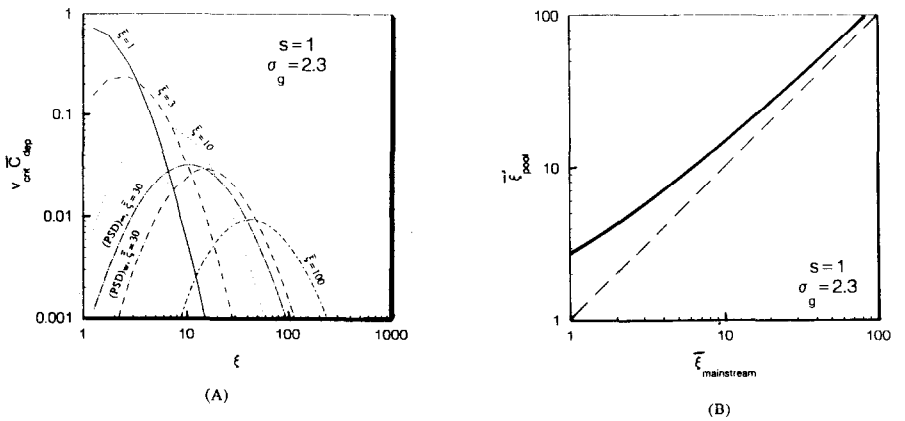

Fig. 12. (A) Pooled deposit particle size distribution on the upwind target surface, and (B) mean particle size in such a distribution [case shown: $\sigma_g = 2.3$, $s = 1$ and $\mathrm{Re}_{p,cr} = 1$].

convective heat transfer reduction associated with fouling layer growth on heat exchanger surfaces.‡‡ Rosner and Tandon (1995) have recently shown that the fractional reduction of convective heat transfer $\dot{q}'_w$ with time t can be formally approximated:

$$\frac{-\Delta\dot{q}'_w}{\dot{q}'_w} \cong \frac{1}{1-\langle\varepsilon\rangle}\frac{\int_0^t (\mathrm{DR})_{ref}\,dt}{d_t}\frac{k_g}{k_{dep}}\cdot\left[\frac{\frac{1}{2}\mathrm{Nu}_h\{0\}}{\mathrm{Nu}_h\{0\}}\right]\cdot\bar{D}_h \tag{30}$$

where $\langle\varepsilon\rangle$ is the average void fraction in the deposit, $(\mathrm{DR})_{ref}$ is the reference deposition rate $(=(\bar{v}N_p U)_{\infty})$ (which can be slowly varying), k_g and k_{dep} are the thermal conductivities of the gas the deposit respectively. Nu_h is the heat transfer Nusselt number and $\bar{D}_h$ is the

‡‡ A similar statement can be made for *radiation* heat transfer since the absorptivity of the layer will generally also be $(\mathrm{PSD})_w$-dependent.

dimensionless, Nusselt number-weighted, upwind surface-averaged deposition rate defined and calculated for different sticking laws in Rosner and Tandon (1995) and Rosner *et al.* (1994). Thus, to make reliable predictions of convective heat transfer reductions, rational estimates of the local granular deposit solid fraction $(1-\langle\varepsilon\rangle)$ and deposit thermal conductivity (k_{dep}) will generally be necessary. These quantities are often sensitive to the local particle size distribution $(PSD)_w$, which we calculate here.

For "sampling" applications the local size distribution formulation and results obtained/discussed here can be used to solve the canonical "inverse" problem—i.e. inferring the corresponding mainstream particle size distribution ($(PSD)_\infty$) based on the observed deposit particle size distribution ($(PSD)_w$) by correcting for aerodynamically induced distortions, position dependence and particle rebound behavior. In terms of equation (21), this is equivalent to solving the indicated integral equation for the "unknown" function $C_\infty\{\xi\}$, having measured the $(PSD)_w$: $C_{dep}\{\xi, \theta\}$, and knowing the local dimensionless impaction frequency $\eta_{loc}\{\xi, \theta\}$ and capture fraction law: $s\{V_p\{\xi, \theta\}/U; \theta_i\{\xi, \theta\}\}$. By differentiating with respect to ξ and formally integrating the result between some convenient reference value $\xi_{ref} > 1$ and any larger ξ-value we find that $C_\infty\{\xi\}$ can, in principle, be constructed from:

$$\frac{C_\infty\{\xi\}}{C_\infty\{\xi_{ref}\}} = \frac{s\{\xi_{ref}, \theta\}}{s\{\xi, \theta\}} \frac{\eta_{loc}\{\xi_{ref}, \theta\}}{\eta_{loc}\{\xi, \theta\}} \frac{C_{dep}\{\xi, \theta\}}{C_{dep}\{\xi_{ref}, \theta\}} \tag{31}$$

an interesting and simple result which should, of course, be independent of the location θ of the $(PSD)_w$-data used or the value of $\xi_{ref} > 1$ chosen. In effect, then, this is a formal direct solution to the inverse problem of constructing the PSD_∞: $C_\infty\{\xi\}$ from local $(PSD)_w$ data: $C_{dep}\{\xi, \theta\}$-data, at least for $\xi \geqslant \xi_{ref} > 1$ and to within a multiplicative constant $C_\infty\{\xi_{ref}\}$.[§§] Needless to say, this procedure imposes no restrictions on the *shapes* of either PSD_∞ or $(PSD)_w$. However, we remind the reader that the accuracy of the inertial impaction correlations which underlay our calculations of $\eta_{loc}\{\xi, \theta\}$ and, implicitly, $s\{\xi, \theta\}$, degrades in the immediate vicinity of the critical Stokes number $Stk_{eff,cr} = 1/8$ (i.e. near $v = v_{cr}$ or $\xi = 1$) (Rosner *et al.*, 1994). Until corrected using rational asymptotic expansions valid near $Stk_{eff,crit}$ (Fernandez de la Mora, 1981, 1984), this fact should be taken into account in selecting the above mentioned value for $\xi_{ref} > 1$.

In Fig. 11 we illustrate the construction of the distribution $C_\infty\{v\}$ from $C_{dep}\{v\}$-data. In this figure, the solid curve corresponds to that portion of the mainstream distribution which *can* be reconstructed and the broken line is the remainder of mainstream distribution. For the constant sticking fraction case, at locations away from the forward stagnation point, smaller particles in the mainstream are incapable of impacting/depositing. Thus, information about mainstream particles *unable to impact* inertially is "lost" and this part of the mainstream distribution cannot be reconstructed from the available $(PSD)_w$-data (Fig. 11). For impact on smooth, solid surfaces, besides the small particles unable to impact, there are much larger particles which do not deposit because they *rebound* upon impact at higher (normal) velocities. For such a case, only a "slice" of the mainstream distribution can be reconstructed from $(PSD)_w$-data (Fig. 11). While $(PSD)_w$-data at any one location on the target may lead to such a "gap" in the inferred supercritical portion of $C_\infty\{v\}$ (Fig. 11) (set by the local rebound of these particles) this gap can be filled, at least partially, with the help of $(PSD)_w$-data from other sampling locations on the same overall target (body) and/or $(PSD)_w$-data from another, independent target of a different diameter exposed to the same mainstream.

Because local size distributions are often sensitive to the nature of the single particle capture law the observed $(PSD)_w$ obtained under known test conditions (including PSD_∞ could, in principle, be used to extract rational estimates of the nature of the sticking law and/or a relevant parameter contained therein; e.g. the dimensionless *rebound parameter*

[§§] To determine this constant and, hence, absolute $C_\infty\{v\}$-values, from the normalization condition $\int_0^\infty C_\infty\{v\}dv = 1$ *will* require a PSD_∞ *shape* assumption for the inaccessible subcritical region $0 \leqslant v \leqslant v_{crit}$.

$U/V_{cr}\{v_{cr}\}$. In the absence of reliable single particle capture data (e.g. $V_{p,cr}\{v, \theta_i\}$; Fig. 2, Wang and John, 1988) for the materials in question, this might be a reasonable provisional method for making extrapolations to other environmental conditions, including predicting deposit properties of more complex-shaped solid surfaces fabricated from the same solid material. Put another way, only the "correct" capture/rebound law will allow the same $C_\infty\{v\}$ distribution to be constructed from $(PSD)_w$-data obtained at all target locations.

5. CONCLUSIONS AND FUTURE WORK

By combining the essential features of single particle sticking probability laws $s\{V_p, \theta_i\}$ with what is now known about particle inertial impaction on a circular cylinder target in high Reynolds number crossflow, we have developed and illustrated here an efficient method to predict the local size distribution of deposited particles. While our illustrative results cover the anticipated dimensionless parameter ranges of current interest, the required formulae are also provided to deal with more complex cases of particular interest to the reader.

Perhaps not surprisingly, the local size distribution of particles in deposits can be significantly distorted when compared with the particle size distribution (here taken to be log-normal) in the mainstream. Indeed, in some cases they are distorted to such an extent that it is not feasible to characterize them even approximately as log-normal (e.g. in the case of deposition on clean-smooth solid surfaces at high values of the rebound parameter, $U/V_{cr}\{v_{cr}\}$). For the case of an impact velocity- and angle independent-(constant) sticking coefficient, the $(PSD)_w$ spread for large values of $\bar{\xi}_\infty$ is approximately the same as the spread of the mainstream distribution, while the mean volume in the deposit distribution is higher than the mean volume in the mainstream. Populations sampled on granular coated surfaces are predicted to have smaller spreads and smaller mean particle size than the corresponding values in the mainstream. Generally, $(PSD)_w$-spreads decrease while mean particle sizes increase at higher angular positions, θ from the forward stagnation point.

Our formulation also leads to a simple solution of the "inverse" (canonical sampling) problem—i.e. that of constructing (a predictable fraction of) PSD_∞ from a knowledge of $(PSD)_w$, the local impingement efficiency function and the operative capture (or rebound) law.

To predict, say, the convective and/or radiative heat transfer reduction associated with fouling layer growth on heat exchanger surfaces, besides local particle *deposition rates* (Rosner and Tandon, 1995; Rosner *et al.*, 1995) and particle size distributions (computed here), information about the *deposit morphology* will be required to determine the thermal and radiative properties of the deposit (e.g. Tassopoulos *et al.*, 1988); Tassopoulos and Rosner, 1995). This level of information will usually require computationally intensive micromechanical modelling at the individual particle level (Konstandopoulos, 1991; Rosner *et al.*, 1992, 1994). Such work is currently in progress. We are also extending our theoretical methods to predict local deposition rates and size distributions for particles deposited by inertial impaction from *spatially nonuniform* and polydispersed particle-laden streams, as often encountered in sampling (Geller *et al.*, 1993) and engineering applications.

Acknowledgements—This research was supported by AFOSR(Grant 94-1-0143; J. M. Tishkoff, Technical monitor) and, in part, DOE-PETC (Grant DE-FG-2290PC90099 (completed Oct. 31 1994; James D. Hickerson, Technical monitor), as well as Yale HTCRE Laboratory *Industrial Affiliate*: Dupont. It is also a pleasure to acknowledge helpful discussions and/or correspondence with J. Fernandez de la Mora, S. W. Rosner and M. J. Labowsky.

REFERENCES

Cheng, Y. and Yeh, H. C. (1979) Particle bounce in cascade impactors. *Environ. Sci. Technol.* **13**(11), 1392.

Dahneke, B. (1971) The capture of aerosol particles by surfaces. *J. Colloid Interface Sci.* **37**(2), 342–353.

Fernandez de la Mora, J. (1981a) Deterministic and diffusion mass transfer mechanisms in the capture of vapors and particles. Ph.D. dissertation, Yale University Graduate School.

Fernandez de la Mora, J. (1984) Asymptotic expansions to predict inertial impaction phenomena in the immediate vicinity of the critical Stokes number. HTCRE Lab. Tech. Report, Yale University.

Fernandez de la Mora, J. (1984) Asymptotic expansions to predict inertial impaction phenomena in the immediate vicinity of the critical Stokes number. HTCRE Lab. Tech. Report, Yale University.

Fernandez de la Mora, J. and Rosner, D. E. (1981) Inertial deposition of particles revisited and extended: Eulerian approach to a traditionally Lagrangian problem. *J. PhysicoChemical Hydrodynamics* **2,** 1–21.

Friedlander, S. K. (1977) *Smoke, Dust and Haze—Fundamentals of Aerosol Behavior.* Wiley, New York.

Geller, A., Rader, D. and Kempka, S. (1993) Calculation of particle concentrations around aircraft-like geometries. *J. Aerosol Sci.* **24,** 823–834.

Israel, R. and Rosner, D. E. (1983) Use of generalized Stokes number to determine the aerodynamic capture efficiency of non-Stokesian particles from a compressible gas flow. *Aerosol Sci. Technol.* **2,** 45–51.

John, W., Fritter, D. N. and Winklmayr, W. (1991) Resuspension induced by impacting particles. *J. Aerosol Sci.* **22,** 723.

John, W. and Sethi, V. (1993) Threshold for resuspension by particle impacting. *Aerosol Sci. Technol.* **19,** 69–79.

Khalil, Y. and Rosner, D. E. (1995) Erosion rate prediction technique for ceramic surfaces in high-speed crossflow of abrasive suspensions. *Wear* (submitted).

Kho, T., Rosner, D. E. and Tandon, P. (1995) Simplified erosion rate prediction technique for cylindrical metal targets in high-speed crossflow of ceramic suspensions. *J. Powder Technol.* (submitted).

Kim, Y. J. and Kim, S. S. (1991) Particle size effects on the particle deposition from non-isothermal stagnation point flows. *J. Aerosol Sci.* **22,** 201–214.

Konstandopoulos, A. G. (1991) Effects of particle inertia on aerosol transport and deposit growth dynamics. Ph.D. dissertation, Yale University Graduate School.

Konstandopoulos, A. G., Labowsky, M. J. and Rosner, D. E. (1993) Inertial deposition of particles from potential flows past cylinder arrays. *J. Aerosol Sci.* **24,** 471–483.

Miller, E., Yarin, A. L. and Goldman, Y. (1992) Competition between thermophoretic deposition and erosion leading to appearance of steady coating. *J. Aerosol Sci.* **23,** 97.

Raabe, O. (1971) Particle size analysis utilizing grouped data and the log-normal distribution. *J. Aerosol Sci.* **2,** 289–303.

Rosner, D. E. (1986) *Transport Processes in Chemically Reacting Flow Systems.* Butterworth Heinemann, Stoneham, MA; Third Printing December 1990. (For fourth printing contact author directly).

Rosner, D. E. (1989) Total mass deposition rates from 'polydispersed' aerosols. *A.I.Ch.E. J.* **35,** 164–167.

Rosner, D. E. and Fernandez de la Mora, J. (1982) Correlation and prediction of thermophoretic and inertial effects of particulate deposition from non-isothermal turbulent boundary layers. In *Particulate Laden Flows in Turbomachinery* (Edited by Tabakoff, W., Crowe, C. T. and Cale, D. B.), pp. 85–94. ASME, New York.

Rosner, D. E. and Fernandez de la Mora, J. (1984) Boundary layer effects on particle impaction and capture. *ASME Trans.-J. Fluid Engng* **106,** 113–114.

Rosner, D. E., Konstandopoulos, A. G., Tassopoulos, M. and Mackowski, D. W. (1992) Deposition dynamics of combustion generated particles: summary of recent studies of particle transport mechanisms, capture rates and resulting deposit microstructure properties. *Proc. Engrg. Foundation Conf., Inorganic Transformations and Ash Deposition During Combustion,* pp. 585–606. ASME/Engrgr. Foundation, New York.

Rosner, D. E., Mackowski, D. W. and Garcia-Ybarra, P. (1991) Size and structure insensitivity of the thermophoretic transport of aggregated 'soot' particles in gases. *Combust. Sci. Technol.* **80**(1–3), 87–101.

Rosner, D. E. and Tandon, P. (1995) Rational prediction of inertially-induced particle deposition rates on a cylindrical target in a dust-laden stream. *Chem. Engng Sci.* **50,** 3409–3431.

Rosner, D. E., Tandon, P., Konstandopoulos, A. G. and Tassopoulos, M. (1994) Prediction/correlation of particle deposition rates from dilute polydispersed flowing suspensions and the nature/properties of resulting deposits. *Proc. 1st Int. Particle Technology Forum,* Vol. 2, pp. 374–381. AIChE, Denver, CO.

Rosner, D. E., Tandon, P. and Labowsky, M. J. (1995) Rapid estimation of cylinder erosion rates in abrasive dust-laden streams. *A.I.Ch.E. J.* **41,** 1081.

Rosner, D. E. and Tassopoulos, M. (1989) Deposition rates from 'polydispersed' particle populations of arbitrary spread. *A.I.Ch.E. J.* **35**(9), 1497–1508. [NB: In this paper following typographical errors should be corrected: Under equation (14) $v/D_p \approx v^{+1/3}$, in the abscissae of Figs 5, 6, 7 and 11 replace v by $\bar{v}$; in equation (30) replace $(1/\bar{v})$ by $(1/\bar{v}^2)$ and in equation (A5) replace μ_k by μ_q. Finally, in equation (A7) add $\equiv$ after μ_q].

Rosner, D. E. and Tassopoulos, M. (1991) Correction for sampling errors due to coagulation and wall loss in laminar and turbulent tube flow: direct solution of canonical 'inverse' problem for log-normal distributions. *J. Aerosol Sci.* **22,** 843–867.

Tandon, P. (1995) Transport theory for particles generated in combustion environments. Ph.D. dissertation, Chemical Engng Dept, Yale University Graduate School.

Tassopoulos, M. (1991) Relationships between particle deposition mechanism and resulting deposit microstructure/effective transport properties. Ph.D. dissertation, Chemical Engng Dept, Yale University Graduate School.

Tassopoulos, M., O'Brien, J. A. and Rosner, D. E. (1988) Simulation of microstructure-mechanism relationships in particle deposition. *A.I.Ch.E. J.* **35,** 967–980.

Tassopoulos, M. and Rosner, D. E. (1995) The effective thermal conductivity of anisotropic packings of spheres. *Chem Engng Sci.* (submitted).

Wall, S., John, W., Wang, H. C. and Goren, S. L. (1990) Measurements of kinetic energy loss for particles impacting surfaces. *Aerosol Sci. Technol.* **12,** 926.

Wang, H. C. (1986) Theoretical adhesion efficiency for particles impacting a cylinder at high Reynolds number. *J. Aerosol Sci.* **17,** 827–837.

Wang, H. C. and John, W. (1988) In *Particles on Surfaces I: Detection, Adhesion and Removal* (Edited by K. L. Mittal), p. 211. Plenum, New York.

Wessel, R. A. and Righi, J. (1988) Generalized correlations for inertial impaction of particles on a circular cylinder. *Aerosol Sci. Technol.* **9,** 26–60.

Xu, M., Willeke, K., Biswas, P. and Pratsinis, S. E. (1993) Impaction and rebound of particles at acute incident angles. *Aerosol Sci. Technol.* **18,** 143–155.